Subnanosecond delay of light in $Cd_xZn_{1-x}Te$ crystals

T. Godde,[1] I. A. Akimov,[1,2,*] D. R. Yakovlev,[1,2] H. Mariette,[3] and M. Bayer[1,2]
[1]*Experimentelle Physik II, Technische Universität Dortmund, 44221 Dortmund, Germany*
[2]*A.F. Ioffe Physical-Technical Institute, Russian Academy of Sciences, 194021 St. Petersburg, Russia*
[3]*CEA-CNRS group "Nanophysique et Semiconducteurs," Institut Néel, CNRS–Université Joseph Fourier, 25 Avenue des Martyrs, 38042 Grenoble, France*

(Received 10 July 2010; revised manuscript received 20 August 2010; published 29 September 2010)

We study the excitonic polariton relaxation and propagation in bulk $Cd_{0.88}Zn_{0.12}Te$ crystals using time-resolved photoluminescence and time-of-flight techniques. Propagation of picosecond optical pulses through a 745-μm-thick crystal results in time delays up to 350 ps, depending on the photon energy. Optical pulses with 150 fs duration become strongly stretched while moving through the sample. The spectral dependence of the group velocity is consistent with the dispersion of the lower excitonic polariton branch. The lifetimes of excitonic polaritons in the upper and lower branches are 1.5 ns and 3 ns, respectively.

DOI: 10.1103/PhysRevB.82.115332 PACS number(s): 71.36.+c, 78.47.D−, 78.40.Fy

When the energy of a photon is close to that of an exciton resonance in a semiconductor its group velocity for propagation through the crystal may be significantly decreased. This phenomenon originates from the strong exciton-photon interaction, which can be treated in terms of an excitonic polariton (EP) quasiparticles.[1–3] The EP propagation and its dispersion have been widely studied in different semiconductor materials[1,4–12] using various experimental techniques. Time-of-flight measurements with pulsed lasers in conjunction with time-resolved detection resulted in group index measurements up to several thousand in GaAs, CuCl, and CdSe crystals.[4–6] In some materials such as anthracene, light may propagate even at velocities below that of sound.[7] Additionally several coherent effects may take place during the optical pulse propagation. In the linear regime interference between the lower polariton (LP) and upper polariton (UP) branches leads to a beating signal, first observed for the 1S quadrupole exciton in Cu_2O.[8] Nonlinear effects such as self-induced transparency at the A exciton in CdSe and at the bound exciton in CdS were also studied using frequency-resolved gating[9] and bandwidth-limited time-resolved spectroscopy,[10] respectively.

Many of the experiments on EP propagation in direct band-gap semiconductors such as GaAs, CdSe, or CdS were performed for resonance conditions on relatively thin crystals (with thicknesses below tens of micron).[1,4,6,9,10] In this case, the EP in both the lower and upper branches propagates through the crystal without significant losses. The group velocity is reduced thousand times but still the optical delay is in the range of several to tens of picoseconds only. It is also known that the EP energy relaxation within the lower branch is strongly suppressed due to the phonon bottleneck in the relaxation path.[13] This effect may be used for long-distance coherent EP propagation and long-time delays of optical pulses. Recently delays of light in the order of several hundreds of picoseconds were reported for 1-mm-thick GaN crystals.[12] Here we report on the direct measurement of subnanosecond optical pulse delays in (Cd,Zn)Te crystals which occur during the propagation of EPs in the lower polariton branch. High-quality samples with low-impurity concentrations result in significant transmission levels in crystals with about 1 mm thickness. The detected group velocity is only 150 times smaller than the speed of light but the resulting time delay accumulated in the crystal can reach almost half a nanosecond. The delay is pronounced at low temperatures $T \leq 25$ K but disappears with temperature increase due to enhancement of EP scattering on acoustical phonons.

In a single oscillator model, the dependence of the dielectric function on optical frequency ω and wave vector k is given by

$$\epsilon(\omega,k) = \epsilon_B + \frac{f\omega_0^2}{\omega_0^2 - \omega^2 + (\hbar k^2/M)\omega_0 - i\omega\Gamma}, \qquad (1)$$

where ϵ_B is the background dielectric constant, f is the oscillator strength, ω_0 is the resonance frequency, M is the exciton effective mass, and Γ is the exciton damping.[14] Solution of $\epsilon=(ck/\omega)^2$ gives the dispersion relation for the transversal EP modes, comprising the LP and UP branches. Here c is the speed of light in vacuum. Obviously, the single oscillator model gives a simplified description for the EP dispersion, especially in zinc-blende crystals such as (Cd,Zn)Te where the band structure is complex.[15] However, as we are mainly interested in the LP branch at optical frequencies $\omega \leq \omega_0$, this simple model gives good agreement with the experimental data. The main parameters for CdTe are known from resonant Brillouin scattering, namely, $\epsilon_B = 11.2$, $f = 8.8 \times 10^{-3}$, and $M = 2.4$ in units of the free-electron mass.[1,16] The energy dispersion curves for the UP and LP branches are plotted in Fig. 1(a) for $\hbar\omega_0 = 1.6638$ eV, neglecting damping ($\Gamma = 0$).

The investigated sample was prepared from an ingot of bulk $Cd_{0.88}Zn_{0.12}Te$ grown by the Bridgman technique at high temperature (1200 °C). The crystal was cut along the (100) plane and after chemical-mechanical polishing had a thickness of 745 μm. The crystal had a very good quality (rocking curve width less than 20 arc sec with an etched pits density of 10^4 cm^{-2}). The crystal was not intentionally doped resulting in slight p-type background doping with a concentration in the order of 10^{15} cm^{-3}.

For time-resolved photoluminescence (PL) and time-of-flight measurements, we used a mode-locked Ti:Sa laser. The laser emitted transform limited pulses with 1 ps or 150 fs

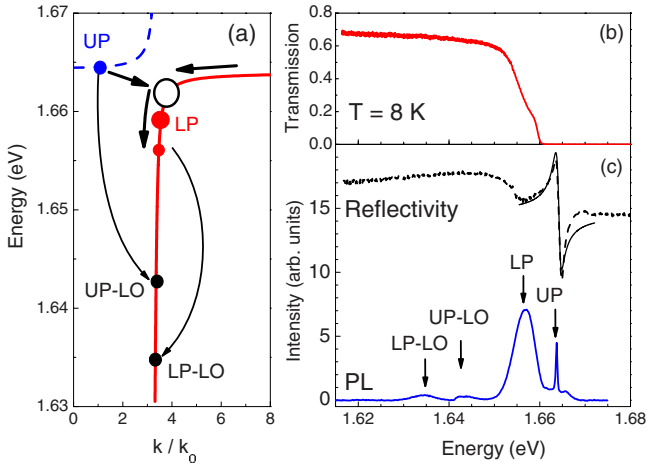

FIG. 1. (Color online) (a) Excitonic polariton energy-wavevector dispersion ($k_0=\omega_0/c$). Circles schematically show EP populations, and arrows indicate relaxation pathways under nonresonant excitation. (b) and (c) Steady-state transmission, reflectivity, and PL spectra at $T=8$ K. PL spectrum was taken under nonresonant excitation ($\hbar\omega_{exc}=2.33$ eV) at pump power density $P=100$ mW/cm^2. Solid line is fit to the reflectivity spectrum with $\hbar\omega_0=1.6638$ eV and $\Gamma=1$ meV (Ref. 17).

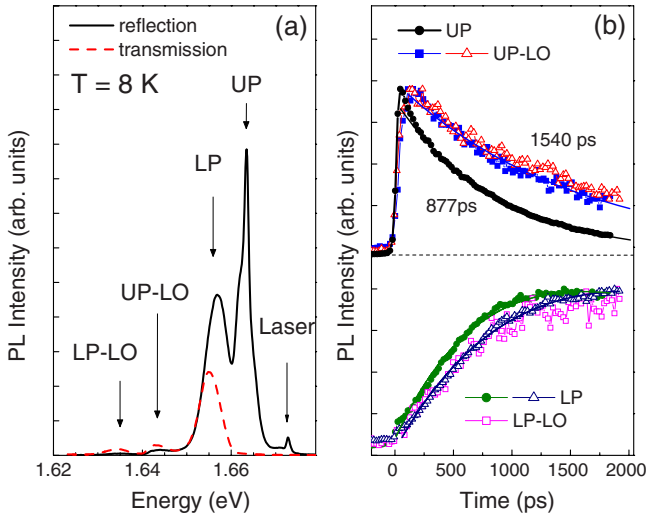

FIG. 2. (Color online) (a) Time-integrated PL spectra under pulsed excitation with pulse duration $\tau_D=1$ ps and $\hbar\omega_{exc}=1.673$ eV in reflection (solid line) and transmission (dashed line) geometry. (b) Intensity transients of UP, LP, and their LO-phonon replicas measured in reflection (full symbols) and transmission (open symbols). Solid lines are exponential fits. The rise times of the LP peaks in reflection and transmission correspond to the decay times of the UP and UP-LO peaks, respectively.

durations at a repetition frequency of 76 MHz. The sample was mounted in a He-bath cryostat with a variable-temperature insert. The PL signal was collected in reflection or transmission geometry. For time-of-flight measurements, the optical pulses hit the sample at normal incidence along the [100] crystallographic axis and the transmitted light was detected. The signal was dispersed by a single 0.5 m spectrometer with 6.28 nm/mm linear dispersion and detected with a streak camera. The overall temporal and spectral resolution of the experimental setup for time-resolved measurements was about 20 ps and 1 nm, respectively. For time-integrated measurements, a nitrogen-cooled charge-coupled-device camera connected to the same spectrometer giving 1.3 nm/mm linear dispersion was used. Steady-state reflectivity and transmission measurements were performed using a halogen lamp. For steady-state PL, we used continuous-wave laser excitation at $\hbar\omega_{exc}=2.33$ eV.

Figures 1(b) and 1(c) show low-temperature ($T=8$ K) time-integrated steady-state transmission, reflectivity, and PL spectra. From reflectivity it follows that the free-exciton resonance is located at $\hbar\omega_0=1.6638$ eV with $\Gamma=1$ meV. In the PL spectrum, the narrow peak at 1.6637 eV is due to radiative emission from the bottom of the UP branch. Consequently the PL maximum of UP is redshifted by 0.66 meV relative to the expected position at $\hbar\omega_0+\Delta_{LT}$, where $\Delta_{LT}=f\hbar\omega_0/2\epsilon_B=0.65$ meV is the longitudinal-transversal splitting. This may be the result of EP localization on alloy fluctuations.[18] The resulting energy fluctuations are, however, small compared to Γ so that we can neglect them. At lower energies, we find a broader peak centered around 1.657 eV, which we attribute to emission from the lower EP branch. The LO-phonon replicas of the UP and LP lines are shifted by $\hbar\omega_{\mathrm{LO}}=22$ meV to lower energies. We observe no PL lines related to donor or acceptor bound excitons, which indicates an exclusively pure crystal quality with a low background impurity concentration.

PL spectra under pulsed excitation with a photon energy of $\hbar\omega_{exc}=1.673$ eV recorded in transmission and reflection geometries are shown in Fig. 2(a). It is important to keep in mind that the EP emission occurs only at the crystal surface where the conversion into photons occurs. The UP branch line is present only in the reflection geometry while the LP peak as well as the phonon replicas of UP and LP are clearly seen in both configurations. This is in accord with the transmission spectrum in Fig. 1(b), where the edge is as well located just below $\hbar\omega_0$. This indicates that polaritons from the lower branch below the phonon bottleneck [indicated by the open circle in Fig. 1(a)] with high probability reach the crystal surface without further scattering. Indeed, if we consider the EP energy relaxation, which is schematically shown in Fig. 1(a), we expect that after the excitation pulse the polaritons in the UP branch either scatter into the LP branch via acoustic-phonon emission or recombine radiatively when they are close enough to the surface. The remaining EPs gather at the knee of the LP branch, where the probability of acoustic phonon scattering is the lowest because of the phonon bottleneck.[13] Finally, they relax further until the group velocity becomes large enough to reach the sample boundary, where they are converted into photons. In case of LO-phonon emission, the EPs always reach the crystal surface and, therefore, the LO replicas in the PL spectrum can be used to monitor the corresponding EP dynamics in the sample volume.[19]

The transients of UP, LP, and their phonon replicas are shown in Fig. 2(b) and confirm the argumentation given above. The UP peak in reflection geometry decays exponentially with a time of 877 ps while its LO replica decays with a 1540 ps time constant, almost twice longer. The latter corresponds to EP scattering into the LP branch. The decay time

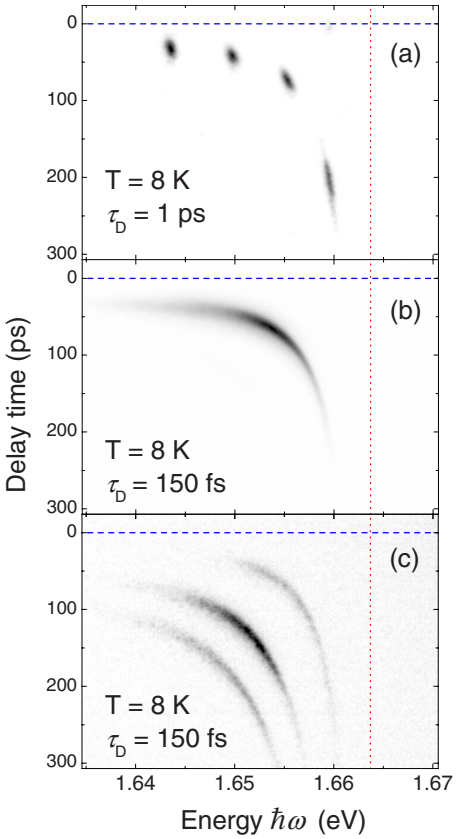

FIG. 3. (Color online) Grayscale contour plots of the intensity of the transmitted optical pulse versus delay time and photon energy for pulse durations of τ_D=1 ps in (a), and τ_D=150 fs in (b) and (c). In (a) data for four optical pulses with different $\hbar\omega_{exc}$ are superimposed. In order to increase the relative intensity of the reflections in (c), the sample was slightly rotated from normal incidence (Ref. 21). Horizontal dashed line indicates zero time and vertical dotted line gives the exciton resonance position $\hbar\omega_0$=1.6638 eV.

of the UP peak may be shorter near the sample boundary due to direct radiative recombination or additional nonradiative recombination at the surface. Note that the UP-LO replica follows the same dynamics in reflection and transmission geometries, monitoring the EP kinetics in the sample volume. The LP peak is expected to have a rise time equal to the UP decay time. This is in full agreement with the experimental data. We fit the LP transients in reflection and transmission with double exponentials where the rise time corresponds to the UP and UP-LO decay, respectively. Good agreement with experiment is obtained for a decay time of about 3 ns, which is attributed to the EP lifetime in the phonon bottleneck region.[13,20] This time constant gives the upper limit for a possible coherent delay of the optical pulse in the LP branch.

After elaborating the EP kinetics, we turn now to the results on optical pulse propagation in the LP branch close to the resonance frequency $\omega \leq \omega_0$. The power density $P \leq 10$ mW/cm^2 was kept low enough to be in the linear regime. The contour plot of the transmitted laser light intensity as a function of delay time and photon energy is presented in Fig. 3. In case of spectrally narrow pulses with durations of τ_D=1 ps, a strong dependence of pulse delay on

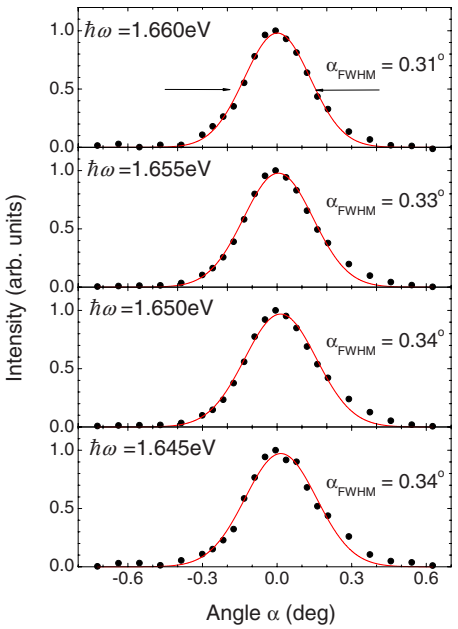

FIG. 4. (Color online) Transmitted beam intensities as functions of the detection angle α for different photon energies $\hbar\omega$. α is taken with respect to the axis normal to the sample surface. Solid lines are fits with a Gaussian distribution.

the photon energy $\hbar\omega_{exc}$ is observed, see Fig. 3(a). The delay time increases when $\hbar\omega_{exc}$ approaches the exciton resonance $\hbar\omega_0$=1.6638 eV. We were able to observe a maximum delay of 350 ps at $\hbar\omega_{exc}$=1.661 eV. The transmission of light at this photon energy decreases drastically and is about 0.2% only.

For short laser pulses with τ_D=150 fs, a strong distortion occurs, see Fig. 3(b). Here, the use of 12 meV spectrally broad pulses centered at 1.653 eV allows one to monitor the EP dispersion in a single measurement. We were also able to detect the subsequent replicas of the pulse, which originate from reflections at the opposite crystal surfaces. The reflections can be seen especially well if the sample is slightly tilted from normal incidence by about 5°, see Fig. 3(c).[21] As expected, the first and second reflections appear at delays which are three and five times larger than the delay of the transmitted pulse. In other words, the pulses propagate over distances of three and five times the crystal thickness of 745 μm.

The propagation of the optical pulses through the crystal is ballistic. This is evidenced by the observation of the reflections. Additionally, we measured the angle distribution of the transmitted beam intensity for different photon energies $\hbar\omega$. These data are presented in Fig. 4. The dependencies can be described by a Gaussian distribution function with a full width at half maximum $\alpha_{FWHM} \approx 0.33°$, that is independent of the excitation energy. Their width is given only by the aperture angle of the incoming focused laser beam. Therefore, we conclude that the photon wave vector is conserved during EP propagation. Assuming that the EP scattering in such pure crystalline samples as the ones studied here is related mainly to inelastic scattering on acoustical and optical phonons, allows us to conclude coherence of the transmitted pulse from the ballistic propagation.

It is clear that the spectral dependence of the time-of-flight signal originates from the strong variation in the group velocity v_g near the resonance frequency ω_0. In order to quantify the experimental results, we have summarized the dispersion relations of the group index $n_g = c/v_g$ and the time delay as a function of the photon energy for different pulse durations τ_D and temperatures in Fig. 5. As expected, the experimental results are independent of pulse duration, i.e., the dispersion curves for $\tau_D = 1$ ps and 150 fs coincide. A temperature increase leads to a redshift of the dispersion curves. Additionally, the transmission efficiency close to the resonance decreases strongly for temperatures above 25 K.

We have calculated the group index according to

$$n_g(\omega) = \frac{c}{v_g(\omega)} = \frac{d}{d\omega}\mathrm{Re}[\omega\sqrt{\epsilon_1(\omega)}], \tag{2}$$

where $\epsilon_1(\omega)$ is the frequency-dependent dielectric function of the LP branch satisfying Eq. (1) and the dispersion equation for transversal modes. The UP branch is not taken into account since the photon energy is below $\hbar\omega_0$. Note that no fitting parameters were used to reproduce the spectral dependence of the group index. As mentioned above, ϵ_B, f, and M are known while ω_0 and Γ are taken directly from the reflectivity measurements at different temperatures, see inset in Fig. 5(b). The results of the calculations are shown by the solid lines in Fig. 5 and are in good agreement with the experimental data. The temperature increase leads not only to a redshift of the energy gap, in correspondence with Varshni's law, but also to an increase in damping Γ, as is clearly seen from the inset of Fig. 5(b). The temperature-induced enhancement of Γ is associated with enhanced EP scattering on acoustical phonons.

In conclusion, we directly observed delays of light pulses by up to 350 ps in a 745-μm-thick (Cd,Zn)Te crystal. The experimental data are well reproduced using the dispersion relation for the lower EP branch calculated in a single oscillator model. From time-resolved measurements, we evaluate EP lifetimes in the upper and lower branches of 1.5 ns and 3 ns, respectively. The realization of large optical delays in ternary alloy crystals such as (Cd,Zn)Te is especially attractive as these systems allow control of the resonance frequency over a broad spectral range from 1.6 to 2.4 eV by tailoring the Zn and Cd contents.

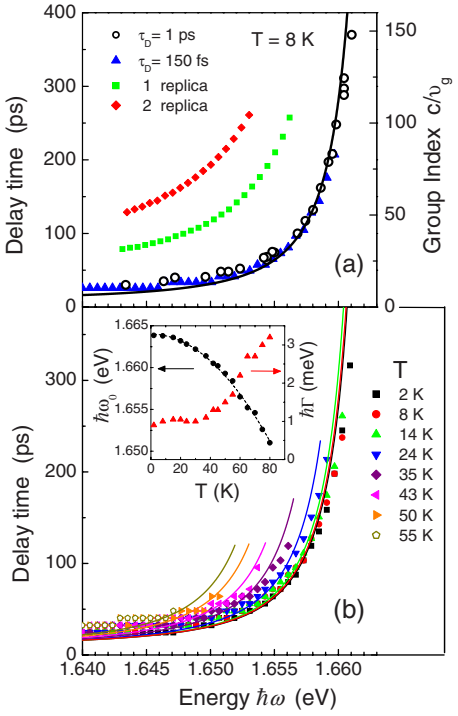

FIG. 5. (Color online) (a) Delay time and group index as functions of optical pulse photon energy $\hbar\omega_{exc}$ for $\tau_D = 150$ fs (solid triangles) and $\tau_D = 1$ ps (open circles). Solid squares and diamonds represent the delay of the first and second reflections, evaluated from Fig. 3(c). (b) Same as (a) but with $\tau_D = 150$ fs for different temperatures. The inset shows the temperature dependencies of resonance energy $\hbar\omega_0$ and exciton damping Γ, as determined from reflectivity spectra and used as input parameters in the group index calculations. Solid lines in (a) and (b) are the delay times calculated with Eqs. (1) and (2).

The authors are grateful to D. Fröhlich, A. N. Reznitsky, and M. M. Glazov for useful discussions.

*ilja.akimov@tu-dortmund.de

[1] E. S. Koteles, in *Excitons*, edited by E. I. Rashba and M. D. Sturge (North-Holland, Amsterdam, 1982), Chap. 3, p. 83.
[2] S. I. Pekar, Zh. Eksp. Teor. Fiz. **33**, 1022 (1957) [Sov. Phys. JETP **6**, 785 (1958)].
[3] J. J. Hopfield, Phys. Rev. **112**, 1555 (1958).
[4] R. G. Ulbrich and G. W. Fehrenbach, Phys. Rev. Lett. **43**, 963 (1979).
[5] Y. Segawa, Y. Aoyagi, and S. Namba, Solid State Commun. **32**, 229 (1979).
[6] T. Itoh, P. Lavallard, J. Reydellet, and C. Benoit à la Guillaume, Solid State Commun. **37**, 925 (1981).
[7] N. A. Vidmont, A. A. Maksimov, and I. I. Tartakovskii, Pis'ma Zh. Eksp. Teor. Fiz. **37**, 578 (1983) [JETP Lett. **37**, 689 (1983)].
[8] D. Fröhlich, A. Kulik, B. Uebbing, A. Mysyrowicz, V. Langer, H. Stolz, and W. von der Osten, Phys. Rev. Lett. **67**, 2343 (1991).
[9] N. C. Nielsen, S. Linden, J. Kuhl, J. Förstner, A. Knorr, S. W. Koch, and H. Giessen, Phys. Rev. B **64**, 245202 (2001).
[10] M. Jütte, H. Stolz, and W. von der Osen, J. Opt. Soc. Am. B **13**, 1205 (1996).
[11] B. Sermage, S. Petiot, C. Tanguy, L. S. Dang, and R. André, J. Appl. Phys. **83**, 7903 (1998).
[12] T. V. Shubina, M. M. Glazov, A. A. Toropov, N. A. Gippius, A. Vasson, J. Leymarie, A. Kavokin, A. Usui, J. P. Bergman, G. Pozina, and B. Monemar, Phys. Rev. Lett. **100**, 087402 (2008).
[13] F. Askary and P. Y. Yu, Phys. Rev. B **28**, 6165 (1983).
[14] E. L. Ivchenko, in *Excitons*, edited by E. I. Rashba and M. D.

Sturge (North-Holland, Amsterdam, 1982), Chap. 4, p. 141.
[15] K. Cho, Phys. Rev. B **14**, 4463 (1976).
[16] R. Sooryakumar, M. Cardona, and J. C. Merle, Solid State Commun. **48**, 581 (1983).
[17] $R=|(1-\bar{n})/(1+\bar{n})|^2$, $\bar{n}=(\sqrt{\epsilon_1\epsilon_2}+\epsilon_B)/(\sqrt{\epsilon_1}+\sqrt{\epsilon_2})$, where $\epsilon_1(\omega)$ and $\epsilon_2(\omega)$ are the frequency dependencies of the dielectric functions corresponding to the LP and UP branches, respectively (Ref. 14).
[18] S. Permogorov and A. Reznitsky, J. Lumin. **52**, 201 (1992).
[19] E. Gross, S. Permogorov, and B. Razbirin, J. Phys. Chem. Solids **27**, 1647 (1966).
[20] D. E. Cooper and P. R. Newman, Phys. Rev. B **39**, 7431 (1989).
[21] Deviation from normal incidence leads to a slight shift of the reflected beams with respect to the optical axis. This allows one to increase the relative intensity of the corresponding replicas by use of spatially selective detection.